

Rice husk ash as an adsorbent for methylene blue—effect of ashing temperature

Sathy Chandrasekhar · P. N. Pramada

Received: 10 August 2005 / Revised: 23 May 2006 / Accepted: 5 July 2006
© Springer Science + Business Media, LLC 2006

Abstract Utilization of one waste material to control pollution caused by another is of high significance in the remediation of environmental problems. Rice husk, an abundantly available agricultural waste, can be used as a low cost adsorbent for dyes and heavy metals in effluent streams. The possible utilization of rice husk ash as an adsorbent for methylene blue dye from aqueous solutions has been investigated. Ash samples from husks of two origins were prepared at different temperatures and their physical, chemical spectroscopic and morphological properties were determined. XRD, FTIR and SEM were some of the techniques adopted for the characterization. The samples were also analyzed for bulk density, pH, nitrogen adsorption properties and lime reactivity. Experiments of methylene blue adsorption on the ash samples were conducted using batch technique and a comparative study was made. Results were analyzed using linear, Langmuir and Freundlich isotherms. The values of separation factor indicate that most of the ash samples do adsorb the dye molecules, but in varying quantities. Calcination at 900°C reduces the adsorption capacity of the ash to a great extent. Regression analysis shows that the experimental data fits both Langmuir and

Freundlich isotherms for certain concentration limits. The adsorbate species are most probably transported from the bulk of the solution into the solid phase through intra-particle diffusion process. Kinetics of adsorption was found to follow pseudo second order rate equation with $R^2 \sim 0.99$. The highest adsorption capacity (Q_0) achieved is found to be ~ 690 mg/g, which is even higher than the values reported for activated carbon from rice husk. The adsorption capacity of the ash samples are in good agreement with their surface area and pore volume.

Keywords Rice husk ash · Silica · Adsorption · Calcination · Methylene blue

Introduction

Environmental pollution and health concerns associated with synthetic dye effluents are well recognized. Regulatory bodies to reduce the quantity of color in effluents and water resources are enforcing increasingly stringent color consent standards. With the growing emphasis on environment-friendly industries, it is important to discover cheap and efficient methods for cleaning industrial wastewater. Various techniques for dye removal have been reported and the advantages and disadvantages have been extensively reviewed (Voudrias et al., 2002 and Valix et al., 2004). Adsorption has been found to be an efficient and economic process to remove dyes, pigments and other colorants and also to control the biochemical oxygen

S. Chandrasekhar (✉) · P. N. Pramada
Regional Research Laboratory (CSIR), Industrial Estate
P.O. Thiruvananthapuram, Kerala, India – 695 019
e-mail: chandrasekharsathy@rediffmail.com

P. N. Pramada
e-mail: pramadapn@yahoo.com

demand. Activated carbon has widely been used for the removal of inorganic and organic pollutants from aqueous solutions because of their high adsorption capacities and amphoteric properties, which enable adsorption of both cationic and anionic dyes. However, cost of production and regeneration of activated carbon is high and its use is unjustified for most pollution control applications (Namasivayam et al., 1998). At this juncture, use of other secondary resource materials becomes highly relevant.

Numerous ligno-cellulosic materials or agricultural wastes such as coconut shell, saw dust, wheat straw, guava seeds, orange peels, bagasse etc. have been considered for the adsorption of dyes (Bhattacharya and Sarma 2003; Sanghi and Bhattacharya, 2002; Kannan and Sundaram, 2002; Manaskorn et al., 2004; Allen et al., 2003; Namasivayam and Kavitha, 2002; Mehment and Mohir, 2003; Waranusantigul et al., 2003; Garg et al., 2004; Rahman and Saad, 2003; Bhattacharya and Sarma, 2005; Senthilkumaar et al., 2005; Annadurai et al., 2002). Conventionally, these materials are pyrolysed or carbonized in an inert atmosphere whereby volatile organic constituents are removed leaving behind a highly porous carbonaceous residue. This material is subjected to either chemical, steam or gas activation (Yupeng et al., 2004). Several studies have been reported to demonstrate the feasibility of adsorption using pyrolysed rice husk (Vadivelan and Vasanth kumar, 2005; Kannan and Sundaram, 2001; Sumanjit and Prasad, 2003; Yupeng et al., 2003; Malik, 2003; Daifullah et al., 2003; Mohamed, 2004; Low and Lee, 1997). The availability of this agro waste at no/low cost makes it more attractive to be used as a raw material for value addition.

Chemical composition of rice husk is found to vary from sample to sample due to difference in type of paddy, crop year, climatic and geographical conditions. Rice husk contains nearly 20% silica with some metallic impurities and the silica content increases to 90% on ashing. Use of chemical fertilizer in paddy field contributes elements like K, Mg, Al, Fe etc. to the rice husk. Various applications of rice husk and its ash has been extensively reviewed (Chandrasekhar et al., 2003). Under controlled conditions, amorphous silica with high reactivity, ultra fine size and large surface area is formed (Chandrasekhar et al., 2002).

Since each form of dye absorbs visible light at a different wavelength, a visible spectroscopic technique has been successfully used to study adsorbent-dye in-

teractions. Methylene blue (basic blue 9/solvent blue 8) has long been used as a model for the adsorption of organic dye from aqueous solutions. Methylene blue is one of the most commonly used thiazine (cationic) dyes and various adsorbents have been reported for its removal from aqueous solutions (Waranusantigul et al., 2003; Garg et al., 2004; Rahman and Saad, 2003; Bhattacharya and Sarma, 2005; Senthilkumaar et al., 2005; Annadurai et al., 2002; Vadivelan and Vasanth kumar, 2005; Kannan and Sundaram, 2001). The present work is a systematic study on the adsorption of methylene blue by ash prepared from two rice husks of different origin at various calcination temperatures. The ash samples were characterized for various properties. Kinetic and equilibrium adsorption studies were conducted and the experimental data were analysed with Linear, Langmuir and Freundlich adsorption isotherms.

Experimental

Materials & methods

Rice husk samples were procured from Kalady ($\sim 10^\circ$ North of equator and 77° East of Greenwich) of Kerala state and Vijayawada ($\sim 15^\circ$ North of equator & 79° East of Greenwich) of Andhra Pradesh state in India and are designated as KRH and APRH respectively. A cationic dye of amorphous nature, methylene blue (MB) of reagent grade having molecular formula $C_{16}H_{18}N_3SCl$ (Mol Wt: 320) with CI No.52015, was chosen as the adsorbate. The rice husks were heated at 300, 500, 700 and 900°C (rate = $5^\circ\text{C}/\text{min}$, holding time = 2 hours) and the ash samples were powdered. The ash samples are designated as KRHT/APRHT where T stands for the ashing temperature.

X-ray diffraction patterns of the ash samples were taken using a Philips X – ray diffractometer (Model X'pert pro) with $\text{CuK}\alpha$ radiation and Ni filter at 40kV and 30mA. The 2 θ step was 0.06 and the step time was 40 sec/step.

Bulk density and pH were determined by following standard procedures. IR spectra were scanned in the range $400\text{--}4000\text{ cm}^{-1}$ in a Perkin Elmer 882 IR spectrometer. The morphology was examined by a scanning electron microscope, JEOL JSM 5600LV (at 20keV with a beam diameter of 20–25 nm).

The surface area, total pore volume, micro pore volume and average pore radius were measured by BET

nitrogen adsorption method at -196°C using Micromeritics Flow Prep 060 model surface area analyzer. The difference between total and micro pore volumes provides the meso pore volume. Micro porous surface area was calculated from the difference between the BET surface area and external surface area. The micro pore volume fraction to the total pore volume is calculated.

The “lime reactivity” of the ash was determined by chemical method (Chandrasekhar et al., 2005). Standard wet chemical methods supported with instrumental techniques were adopted to determine the chemical constituents. The loss on ignition (LOI) was determined by heating the ash at 1025°C for 1 h and calculating the loss in weight. Carbon content in selected samples was determined using Carbon – Sulphur analyzer (Advance Research Instruments, Model C & S) by heating the sample to 1100°C in air and measuring the CO_2 evolved. A reference material with 1% carbon was used as the standard.

Adsorption experiments

Methylene blue solutions of different concentrations were prepared and the absorbance was measured at 668 nm using UV-Visible spectrophotometer (Jenway, UK). A calibration graph was drawn by plotting absorbance against concentration. Adsorption studies were carried out at 30°C under batch mode using a shaking water bath with temperature control (Julabo SW22) at constant agitating speed of 200 rpm. The effect of contact time and initial dye concentration on color removal was studied by a series of kinetic and equilibrium experiments which were always carried out in duplicate and the mean values were taken. The maximum deviation was 3%.

Kinetic studies were conducted where a known quantity of the sorbent was contacted with a dye solution and shaken at 30°C for given recorded time (2, 5, 15, 30, 60 and 120 minutes) The initial concentration of the dye was 50 mg/l and that of sorbent was 2 g/l. Addition of the ash brought down the pH of the methylene blue solution from ~ 7.2 to ~ 6.4 . The contents of each flask were centrifuged (Hettich Centrifuger) at 5000 rpm for 3 min and the absorbance of the solution was measured. The difference in concentration before and after the reaction corresponded to the quantity of the dye adsorbed by the ash. These experiments were used to establish the equilibrium time between the sor-

Table 1 Chemical analysis of the rice husk ash (Chandrasekhar et al., 2005)

Constituents (Wt %/ppm)	KRH	APRH
$\text{SiO}_2 (\pm 0.1)$	94.64	88.47
$\text{Na}_2\text{O} (\pm 0.01)$	0.39	0.26
$\text{K}_2\text{O} (\pm 0.01)$	0.58	2.50
$\text{Fe}_2\text{O}_3 (\pm 0.01)$	0.23	0.40
$\text{CaO} (\pm 0.01)$	1.89	1.80
$\text{MgO} (\pm 0.01)$	0.96	0.71
Zn ppm (± 1)	18.20	32.28
Mn ppm (± 1)	52.24	56.44
Cu ppm (± 1)	32.17	16.98
Cd ppm (± 0.01)	0.48	0.49

bent and the dye solutions. This equilibrium time was used as contact time in the isotherm experiments.

In the equilibrium experiments, dye solutions of different concentrations (5–100mg/l) were contacted with the sorbent (2 g/l) for 30 min in a shaker at 30°C for all samples except for APRH 900 where a time of 2 h was given. In each case a blank experiment (with out dye) was also carried out.

Results and discussion

Characteristics of the ash samples

The ash content of the husk samples are found to be as 17.86 and 19.25 for APRH and KRH respectively. Chemical assay shows that APRH ash contains only 88.47% silica where as the KRH ash has 94.64% (Table 1). Minor constituents such as K_2O and Fe_2O_3 are higher in APRH ash i.e., 2.51, 0.41% respectively compared to 0.59 and 0.24 % in KRH ash. The APRH ash contains small amount of black carbon particles which are formed during surface melting at $\sim 350^{\circ}\text{C}$ due to the presence of low melting K_2O (Chandrasekhar et al., 2005).

The ash samples prepared from KRH and APRH at different temperatures are studied in detail for their properties as well as their adsorption behaviour.

Bulk density

Bulk density is an important characteristic of a carbonaceous product and is related to the nature of its source material. It affects the overall cost of adsorption process. Generally an adsorbent with higher bulk density

Table 2 Properties of ash samples at different temperatures

Sample	LOI % (± 0.2)	pH (± 0.1)	Bulk density g/ml (± 0.01)	Lime reactivity mg CaO/ g ash (± 1)
KRH300	66.3750	4.01	0.35	51.80
KRH500	11.9248	7.91	0.38	189.00
KRH700	1.8261	8.86	0.38	101.33
KRH900	0.6710	7.59	0.40	33.50
APRH300	55.6772	6.05	0.39	24.81
APRH500	8.4588	9.12	0.39	61.49
APRH700	1.4852	8.80	0.39	15.15
APRH900	0.3835	8.45	0.44	16.21

need not be frequently regenerated because it can hold more adsorbate per unit volume. Bulk density values of the ash samples are found to be in the same range (Table 2) except for KRH900 and APRH900. The higher values indicate that some densification has occurred at this temperature.

Lime reactivity

Chemical reactivity of rice husk silica is determined by treating with slaked lime ($\text{Ca}(\text{OH})_2$) and hence is termed as lime reactivity. The amount of Calcium which reacts with silica is directly related to the reactivity and in turn related to the quantity of amorphous silica in the ash. It is also directly related to the surface area of the ash. It has been established that at higher temperatures and soaking times, cristobalite (crystalline form of silica) is formed which has very low reactivity (Chandrasekhar et al., 2005). Table 2 gives the lime reactivity values of the ash samples. The APRH ash samples have lower values than the corresponding KRH ash. Reactivity of the silica/ash can vary due to sintering effects or phase transitions. The minor constituents in husk act as inhibitors when subjected to ashing at higher temperatures. The presence of higher amounts of alkalis in APRH may be attributing to this phenomenon.

XRD analyses

Figure 1 shows XRD patterns of the ash samples from KRH and APRH. All samples except APRH500 and APRH900 show a diffused peak with its maximum at about $2\theta = 22^\circ$ characteristic of amorphous silica. Sharp peaks are observed for APRH500 at $\sim 28^\circ$ and APRH900 at 21.8° which correspond to carbon

(graphite) and cristobalite respectively. The potassium in the APRH causes surface melting and accelerates the crystallization of cristobalite (Krishnarao et al., 2001). Peak corresponding to carbon (in SP^2 hybridized graphite form) is exhibited by only APRH500. Decomposition of the husk may not be starting at 300°C and

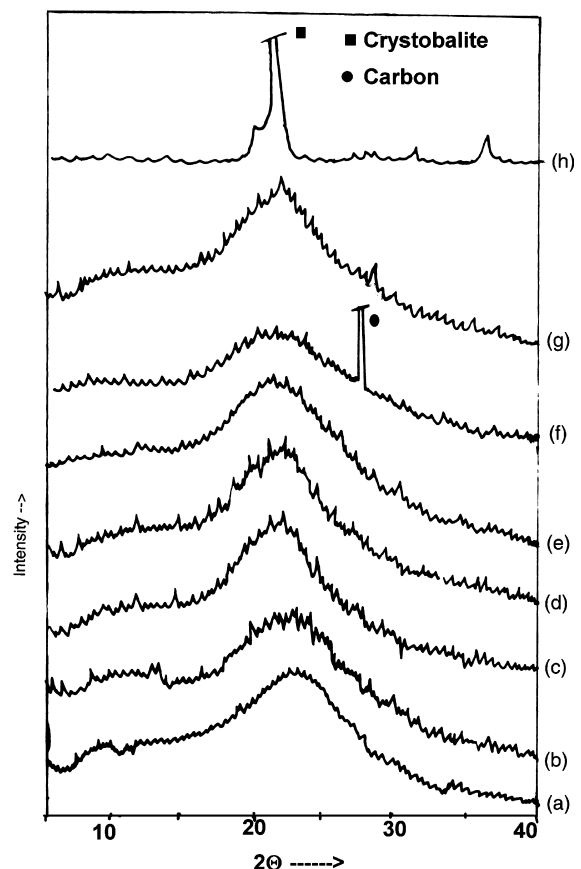


Fig. 1 XRD patterns of the ash samples a- KRH300, b- KRH500, c- KRH700, d- KRH900, e- APRH300, f- APRH500, g- APRH700 and h APRH900

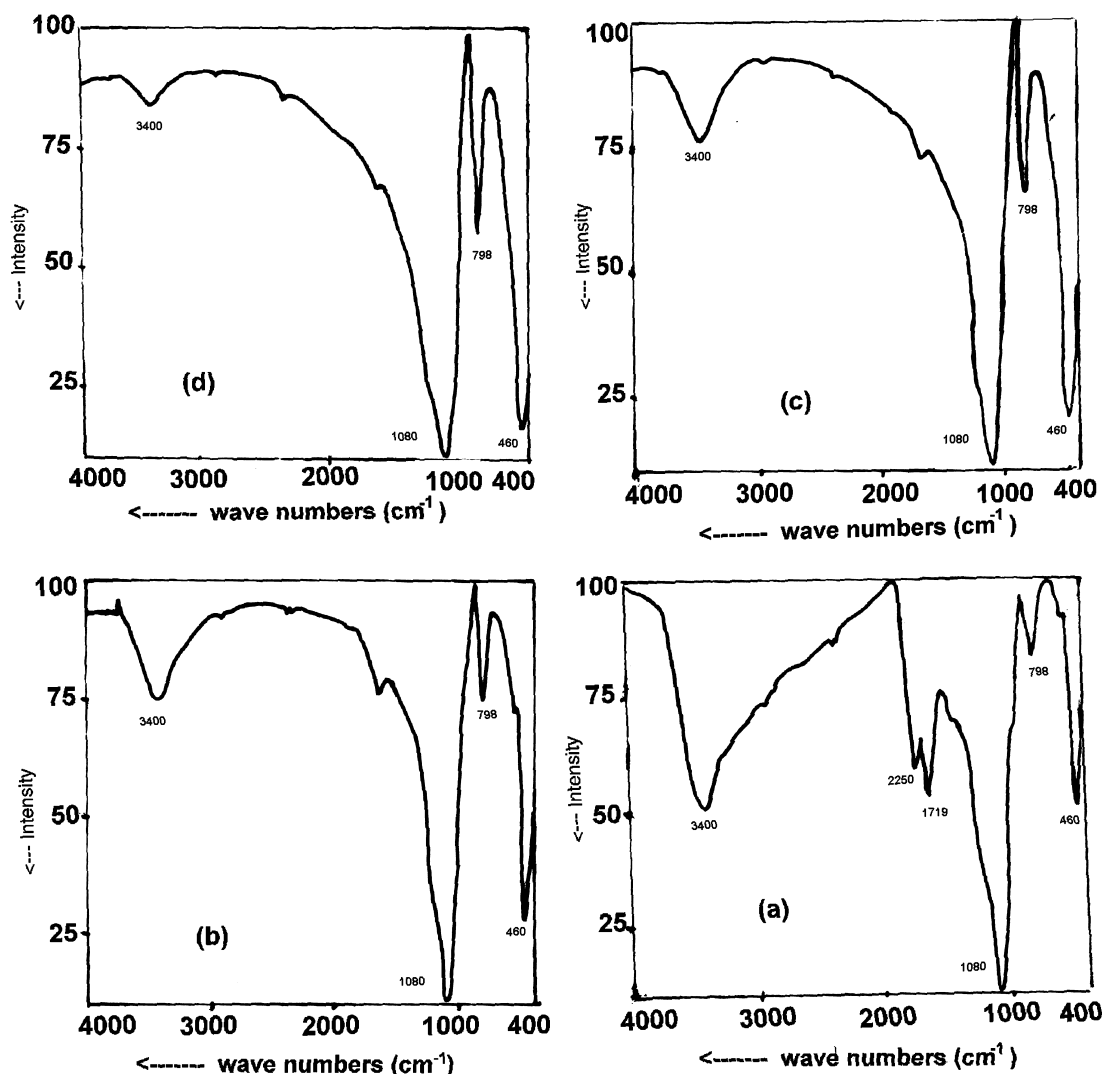


Fig. 2A IR spectra of KRH; a-300, b-500, c-700 and d-900

therefore no peak of carbon is found for APRH300. In KRH samples the % potassium is low and surface melting is insignificant. Hence, the possibility of carbon fixation in KRH ash samples is eliminated and all the carbon formed during the decomposition is oxidized to CO_2 . Since the carbon is not fixed in KRH ash, it is more reactive than that of APRH. The ash samples APRH700 and APRH900 are in a fused state where the carbon is encapsulated. At 900°C both KRH and APRH form crystallite and the adsorption capacity drastically decreases.

KRH500 is having 3.45 % (wt/wt) of carbon where as APRH500 has only 1.52 %. In KRH700 all the car-

bon has escaped as CO_2 and the % carbon is below detectable limit. For APRH 700, carbon is still present (0.23%) but in a fused or fixed state. The carbon estimation results support the XRD data.

IR spectral analyses

Four bands are observed in the FTIR spectra of all samples at around 3400, 1080, 798 and 460 cm^{-1} (Fig. 2A and 2B). The broad bands around 3400 and 1080 cm^{-1} are due to the $-\text{OH}$ vibrations and hence attributable to the existence of surface hydroxyl groups and chemisorbed water (Daifullah et al., 2003 and

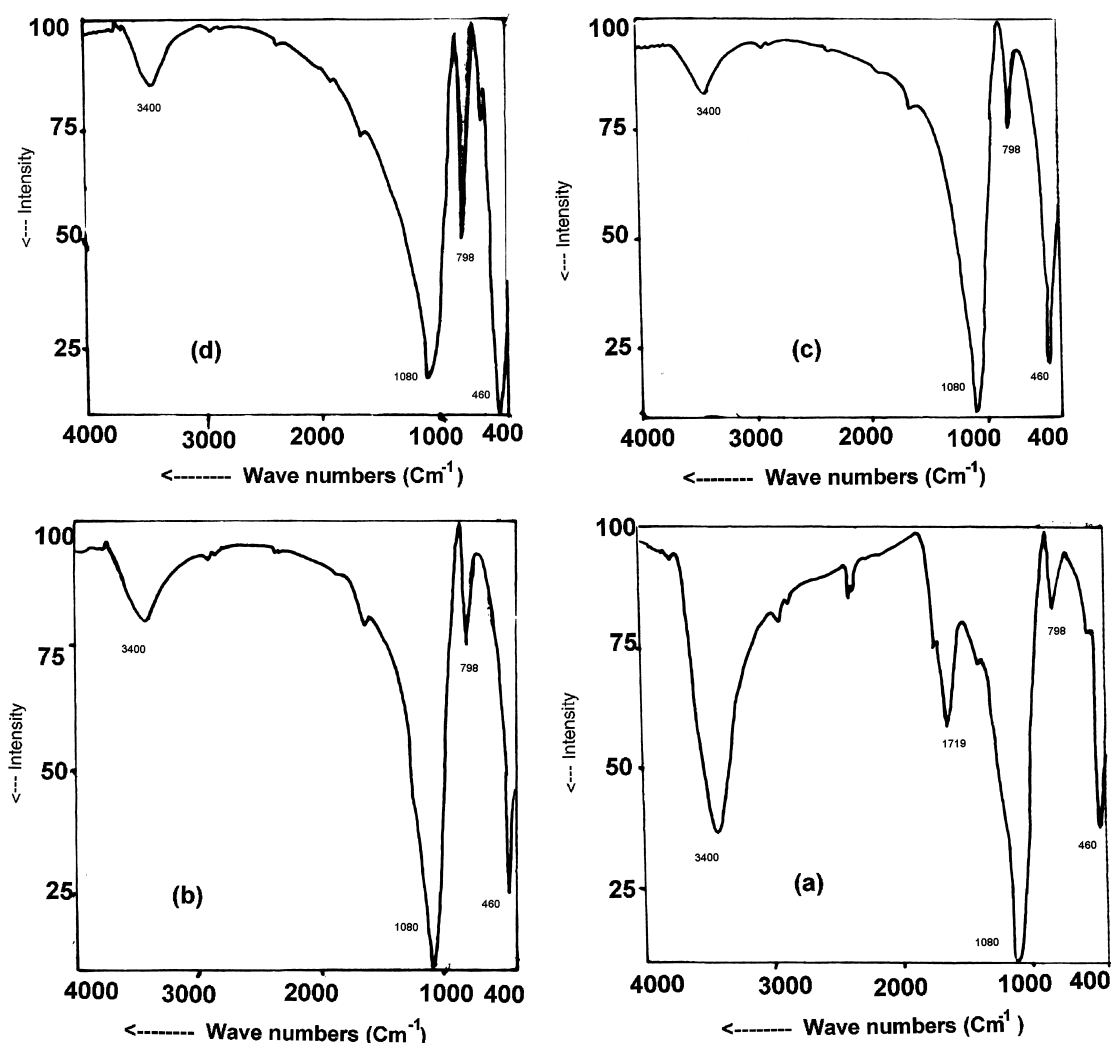


Fig. 2B IR spectra of APRH; a-300, b-500, c-700 and d-900

Ibrahim et al., 1998). Band at 3400 cm^{-1} indicates both free and hydrogen bonded hydroxyl groups. The bands at ~ 1080 and 798 cm^{-1} correspond to O-Si-O stretching and that at $\sim 460\text{ cm}^{-1}$ to bending. The extra bands at ~ 1719 , 2250 cm^{-1} in KRH300 (Fig. 2A) and APRH300 (Fig. 2B) corresponds to C-O stretching vibration of ketones, aldehydes, lactones or carboxyl groups. Intensity of these bands decreases or is almost negligible in ashes at higher temperature and therefore the surface functional group is generally neutral or slightly acidic. The main surface functional groups present in the ash are carbonyl groups. The intensity of the bands at 3440 and 1080 cm^{-1} decreases as the calcination temperature increases. This can be attributed to the decrease of surface hydroxyl groups. The in-

crease in intensity of the bands corresponding to silica (at ~ 798 and 460 cm^{-1}) with calcination temperature is possibly due to the formation of more siloxane groups with increased stretching of Si-O-Si bonds.

Electron microscopic studies

Morphological studies reveal that the ash samples are having particles with varying size (Figure 3A and 3B). In KRH300, the morphology of rice husk is retained with protruding parts damaged slightly and the particle size is up to $500\text{ }\mu\text{m}$ (Figure 3A-a). The particles in KRH500 are finer than those in KRH300 and most of them are below $200\text{ }\mu\text{m}$ (Figure 3A-b). The rice husk skeleton is retained even though it is much more

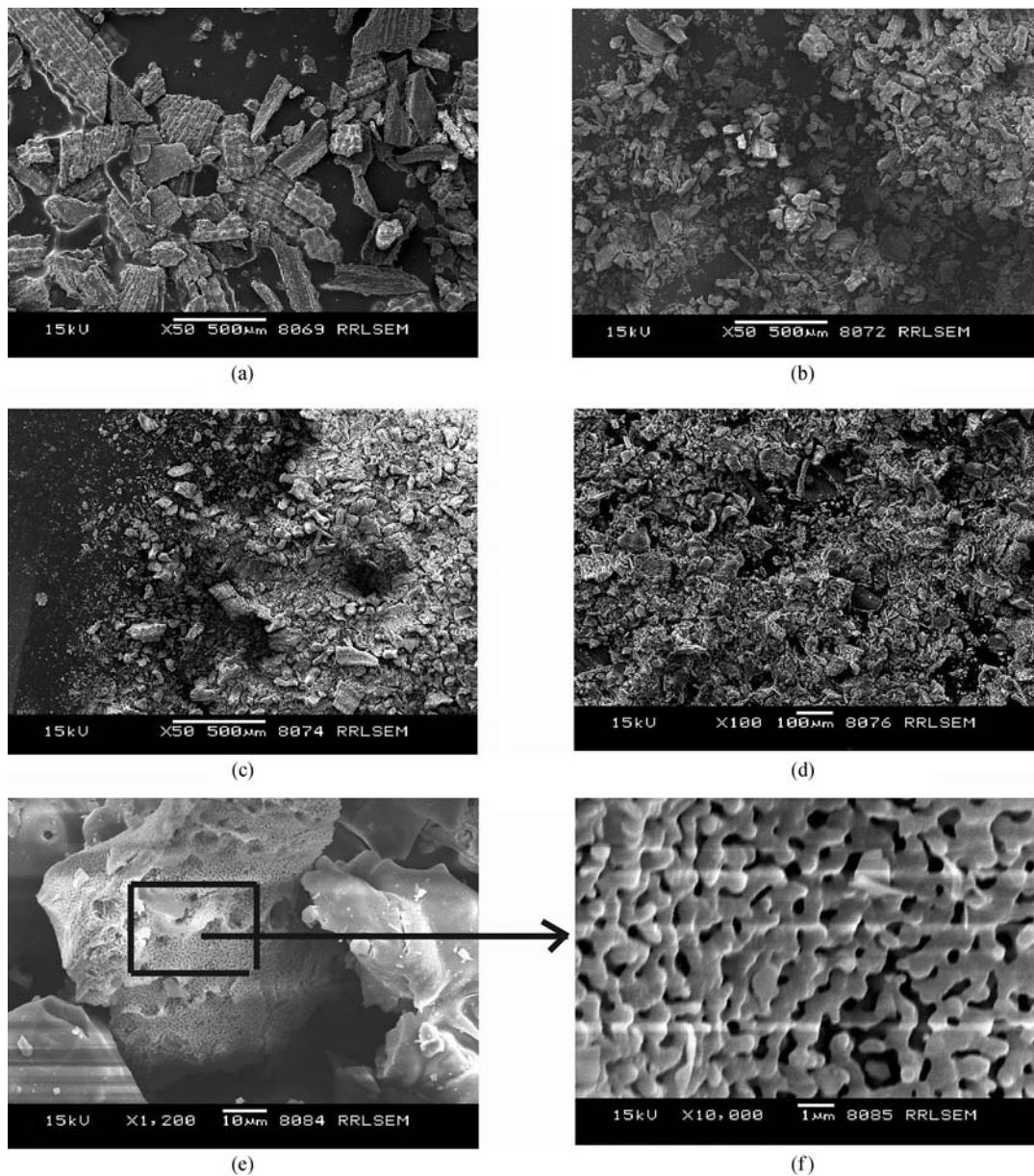


Fig. 3A SEM pictures of KRH ash samples

deformed. Highly porous and fine particles are seen. Small cavities on the surface indicate the presence of interconnected porous net work as evident from the magnified image of KRH500 (Figure 3A-(e) & (f)). The particles in KRH700 are below $100\ \mu\text{m}$ and more fines are present (Figure 3A-(c)). The bigger particles appear to have pores. In KRH900, the particles are much below $100\ \mu\text{m}$ and in a fused state (Figure 3A-d). Surface is smooth and open pores are less which is supported

by the N_2 adsorption data (very low pore volume of KRH900). The particles in APRH300, to a great extent, are of $500\text{--}300\ \mu\text{m}$ size and the morphology of the rice husk is retained (Figure 3B-a). The morphology of APRH500 is similar to that of APRH300 (Figure 3B-b). Some of the particles are having very fine pores $<1\ \mu\text{m}$ size and most of the particles are closely connected to each other. Only a few particles are of size $200\text{--}400\ \mu\text{m}$ in APRH700, and appear to have pores

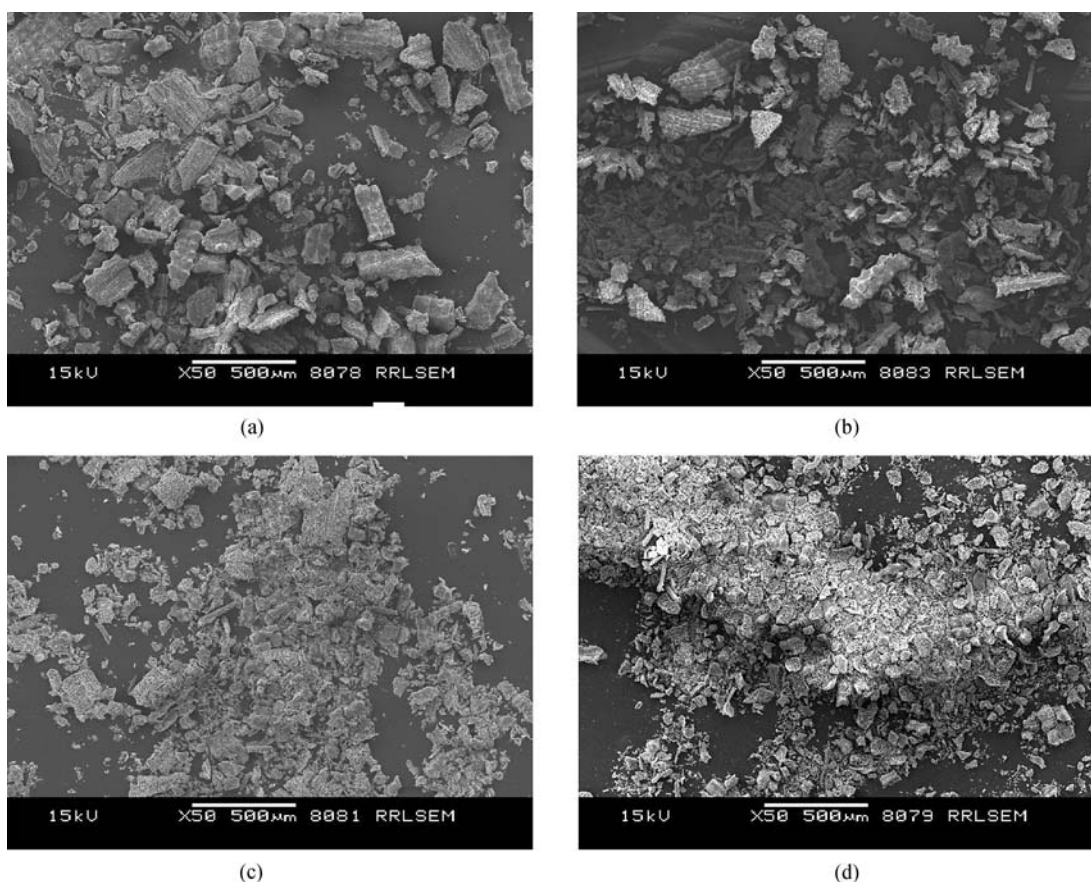


Fig. 3B SEM pictures of APRH ash samples

(Figure 3B-c). In APRH900, all the particles are $<100\ \mu\text{m}$ and are highly deformed (Figure 3B-d).

Nitrogen adsorption properties

Adsorption is a complex phenomenon and many factors can affect this property. Pores within porous materials are generally classified into micro pores ($<2\ \text{nm}$ diameter), meso pores ($2\text{--}50\ \text{nm}$) and macro pores ($>50\ \text{nm}$). The pore structure and the surface chemistry of the ash have significant effect on big molecules like methylene blue (Yupeng et al., 2003). Methylene blue molecule has a minimum molecular cross section of about $0.8\ \text{nm}$ and cannot enter the pores with diameter less than $1.3\ \text{nm}$. Therefore, it can only enter into the larger micro pores (Daifullah et al., 2003). The surface area, total pore volume (meso and micro pores), average pore radius and micro pore surface area of the samples are given in Table 3. These values are highest for KRH500 and lowest for APRH900 and are in line

with their adsorption behaviour. The KRH ash samples have higher surface area and pore volume than APRH except for APRH300.

The surface area of rice husk ash is dependent on the amorphous carbon and silica formed during burning. At 300°C , the burning is incomplete and the rice husk skeleton is not completely destroyed and hence surface area is not high. In APRH, the surface area of the ash decreases with increase in temperature (from 300 to 900°C) because the particles undergo fusion due to surface melting and the pores are partly closed. Crystallization of silica also takes place at higher temperature. In KRH, potassium content is much less and hence the surface melting is reduced (Table 1). As the temperature of ashing is increased to 500°C , the decomposition of organics is more or less complete and maximum amount of carbon along with amorphous silica is formed giving high surface area to the ash. At 700°C , the carbon burns off and the ash is mostly amorphous silica which is transformed to crystalline form at 900°C .

Table 3 N₂ adsorption data

Sample	BET SA m ² /g	Total Pore Vol cm ³ /g	Micro Pore Vol cm ³ /g	Micro pore surface area	micro pore fraction (%)	Meso pore vol	Pore Radius nm
KRH300	11.38	0.0056	0.0003	0.6017	5.36	0.0054	0.9905
KRH500	101.29	0.0465	0.0031	14.4064	6.67	0.0434	0.9173
KRH700	33.48	0.0166	0.0016	3.006	9.64	0.0150	0.9891
KRH900	6.40	0.0031	BDL	—	—	0.0031	0.9680
APRH300	25.07	0.0125	0.0011	2.1054	8.80	0.0114	0.9952
APRH500	14.38	0.0071	0.0003	0.7033	4.23	0.0068	0.9891
APRH700	8.43	0.0041	BDL	—	—	0.0041	0.9738
APRH900	2.85	0.0010	BDL	—	—	0.0010	0.6978

The absence of carbon in KRH700 and agglomeration of particles in the formation of crystalline silica in KRH900 bring down the surface area of these samples. Thus the surface area and pore volume pass through a maximum for KRH series (KRH500) whereas they decrease monotonically in the APRH series.

Surface area does have a major role in dye removal. During the adsorption phenomenon, the dye molecule gets attached to the active sites of the sorbent surface and then it diffuses into the pores. The effect of pore volume on the adsorption is due to the steric hindrance associated with the size of the dye molecule which limits its penetration into the pore structure. Therefore, the adsorption increases with surface area and pore volume of the sorbent.

Loss on ignition

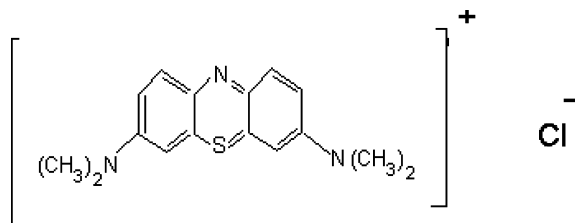
The LOI corresponds to the volatile components as well as the remaining carbon in the ash. Table 2 gives the LOI values of the ash samples. KRH300 and APRH300 are having higher LOI indicating the presence of large amount of carbon/volatiles in these samples. When calcination temperature is increased, LOI of the ash decreases and comes to <1% for sample prepared at 900°C. LOI values confirm the presence of carbon along with silica in KRH and APRH ashes formed at 300 and 500°C. Higher adsorption capacity of KRH500 and APRH500 is due to the presence of both carbon and silica. At higher temperature even though the APRH ash is blackish, the LOI is less which supports the presence of entrapped carbon in the sample.

pH

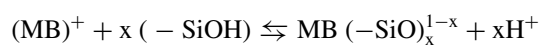
Activated carbons, which are commonly used as efficient adsorbents, are categorized into H and L carbons

according to their pH in a bulk solution (Al-Degs et al., 2000). H carbon adsorbs more H⁺ ions than OH[−] and produces a suspension which has an alkaline property (pH > 7.0) and a positive zeta potential. An L carbon has been shown to produce a bulk acidic suspension and to exhibit a negative zeta potential. It is reported that carbon surfaces acquire a “basic” character upon heat treatment (>700°C). pH value > 7 indicates a negative external surface charge or surface basicity and acidic uptakes.

All the ash samples except KRH300 are having pH ≥ 7 (Table 2) and can attract positively charged species of the methylene blue during the adsorption process. Methylene blue dissociates in aqueous solution as



Hydrogen bonds would be expected to occur between amino group in the dye molecule and the oxygen atoms and hydroxyl groups of the silica surface. The rapid uptake of dye indicates that the sorption process could be ion exchange in nature where the cationic methylene blue reacts with the −OH group eliminating HCl. The ion exchange reaction at the silicon surface is accomplished through the substitution of protons of the surface silanol group by the +ve ion of methylene blue from the solution as follows:



where (MB)⁺ is the positive ion of methylene blue, −SiOH is the silanol group on the ash surface and x is

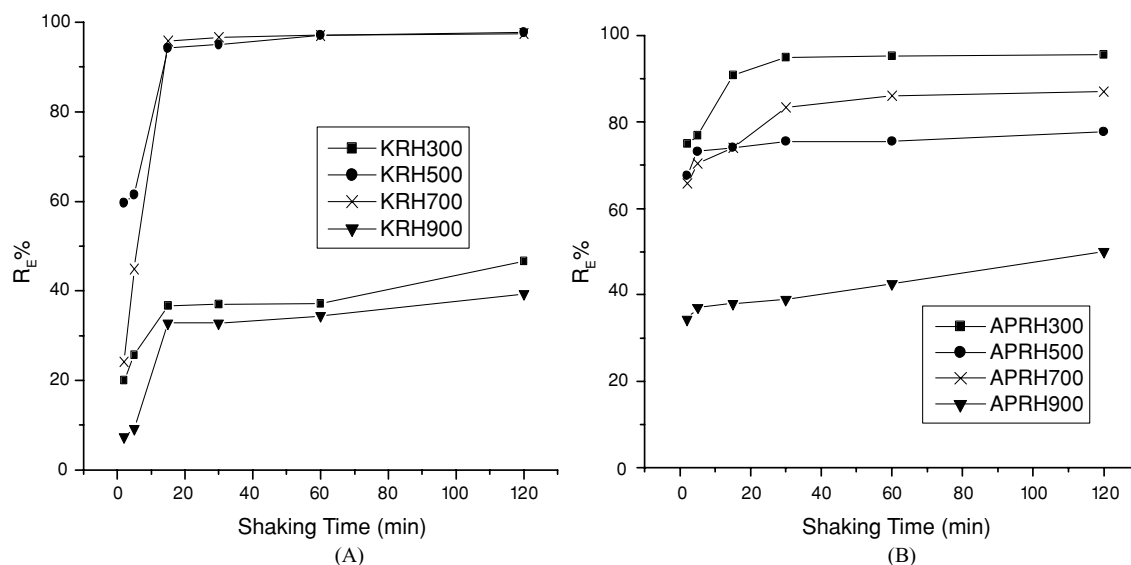


Fig. 4 Removal efficiency versus shaking time for A – KRH and B – APRH

the number of protons released (Daifullah et al., 2003). The pH of the dye solution is ~ 7.2 and addition of the ash was found to bring down the value to ~ 6.4 . The lower adsorption capacity of KRH300 may be due to its lower pH.

Even though the pH has impact on the adsorption capacity, its influence is not as critical as that of surface area and pore volume. For a good adsorbent of methylene blue, its pH should be ≥ 7 and surface area and pore volume should be large. The ash samples KRH500, KRH700, APRH300, APRH500 and APRH700 satisfy these conditions and hence appear to be suitable for methylene blue removal.

Basic dyes upon dissolution release dye cations in the solution. Adsorption of these charged dye groups on to the adsorbent surface is primarily influenced by the surface charge on the adsorbent. The surface of rice husk ash is negatively charged due to the presence of $-\text{OH}$ groups and hence has a high adsorption capacity for cationic (basic) dyes. The higher pH of the ash also supports this. It is primarily the hydroxyl groups that determine the chemistry (acid base character) and reactivity of these surfaces.

Adsorption studies

Kinetics

The effect of contact time on the dye removal of the samples was studied by evaluating the removal effi-

ciency, R_E of the methylene blue calculated as

$$R_E(\%) = [(C_0 - C)/C_0] \times 100 \quad (3)$$

where C_0 is the initial concentration of the dye and C is the solution concentration after adsorption (Rahman and Saad, 2003). Figure 4A and B show the removal efficiency of the samples against shaking time for KRH and APRH ashes respectively.

The adsorption pattern of methylene blue by the ash at different shaking time can be divided into two regions. The first corresponds to a fast removal rate and the second to a slow removal until equilibrium is reached. During adsorption, the dye molecules initially reach the boundary layer, then diffuse into the adsorbent surface and finally, into the porous structure of the adsorbent which contain large number of micro pores. The diffusion on to the external surface was fast followed by slow diffusion into the intra particle matrix finally rapid equilibrium was attained. Hence, this phenomenon will take a longer contact time. Figure 4 reveals that curves are single, smooth and continuous, leading to saturation, and suggests the possible monolayer coverage of methylene blue on the ash surface. Similar results have been reported in literature for the removal of dyes and metal ions from aqueous solutions using various activated carbons (Senthilkumar et al., 2005; Vadivelan and Kumar, 2005).

The relative increase in the removal of dye after a contact time of 30 minutes is not significant for

Table 4 Graphical parameters of KRH and APRH

Samples	Parameters of $\log R_E$ vs $\log t$			Parameters of intra particle diffusion model	
	m	K	R^2	Intercept K_p	R^2
KRH300	0.3010	15.84	0.9989	55.09	0.9999
KRH500	0.2335	47.86	0.9177	480.77	0.9566
KRH700	0.6847	15.13	0.9999	556.38	0.9951
KRH900	0.7525	3.71	0.9442	187.92	0.9110
APRH300	0.0758	62.32	0.9021	509.50	0.8974
APRH500	0.0506	59.84	0.9137	385.42	0.9951
APRH700	0.0854	52.72	0.9779	427.68	0.9956
APRH900	0.0903	26.53	0.9120	187.29	0.9966

all samples except APRH900 and hence the optimum contact time is fixed as 30 minutes. Longer time is required for APRH900 ash to attain the equilibrium concentration, and the optimum time is found to be 2 h (Figure 4B). This is due to the much lower surface area and pore volume of this sample.

KRH500 and KRH700 are having higher removal efficiency than other KRH samples because of their higher surface area and pore volume (Figure 4A). The micro pore surface area is also highest for KRH500. Among the APRH samples, APRH900 has the least removal efficiency. The most promising samples are found to be KRH500, KRH700, APRH300, APRH700 and APRH500 out of which KRH500 and KRH700 are showing maximum removal efficiency. At 900°C, the amorphous silica is converted to crystalline form decreasing the surface area and/or pore volume and hence lowers the adsorption capacity of KRH900 and APRH900. Adsorption capacity is in good agreement with the surface area and pore volume.

The adsorption mechanism of the above data can be expressed in terms of the logarithmic plot of R_E versus shaking time

$$\log R_E = m \log t + \log K \quad (4)$$

where m is the slope and represents the adsorption mechanism and K is a constant and may represent the rate factor (Rahman and Saad, 2003).

Table 4 gives the parameters for $\log R_E$ versus $\log t$ plot. Smaller values of slope m with increase in surface area indicates better adsorption, where as smaller values of K for comparatively lower surface area may be due to the smaller pore volume or active sites in the ash (Rahman and Saad, 2003). In KRH series, the small-

est m value is for KRH500 which is having highest surface area and adsorption capacity. The discrepancy between KRH300 and KRH700 is due to the presence of higher micro pore fraction in KRH700, which account for surface area increase but not for removal of the big methylene blue molecule as given in Table 3. For APRH samples, even though APRH500 is having minimum ' m ' value, its surface area is relatively low. APRH300 with low ' m ' value and higher surface area is therefore having maximum adsorption.

The mismatch in the order of adsorption and ' m ' value for certain APRH samples may be due to surface melting at $\geq 300^\circ\text{C}$. At this stage, a certain amount of fused mass rather than a porous matter is present (Krishnarao et al., 2001). This is the reason for the lower removal efficiency of APRH500 and APRH700 compared to the corresponding KRH samples (Figure 4). The K values of APRH samples are higher than those of KRH but APRH series is having lower surface area than KRH. Adsorption depends on the active sites and the K value is proportional to the active sites, surface area and pore volume. For APRH samples, active sites are more compared to KRH because of the presence of carbon or/and surface -OH groups. Since the APRH ash contains fused matter, the adsorption efficiency is lower. At 300°C, potassium in this ash acts as chemical activator and thus favors the formation of activated carbon. So both silica and active carbon is present in this sample. APRH300 is having higher surface area than KRH300 hence the higher removal efficiency. At 900°C, amorphous silica present in both samples is transformed into cristobalite and the removal efficiency drastically decreases. The removal efficiency and surface area are in good agreement for KRH series but not for APRH500 and APRH700 due to the reasons mentioned earlier.

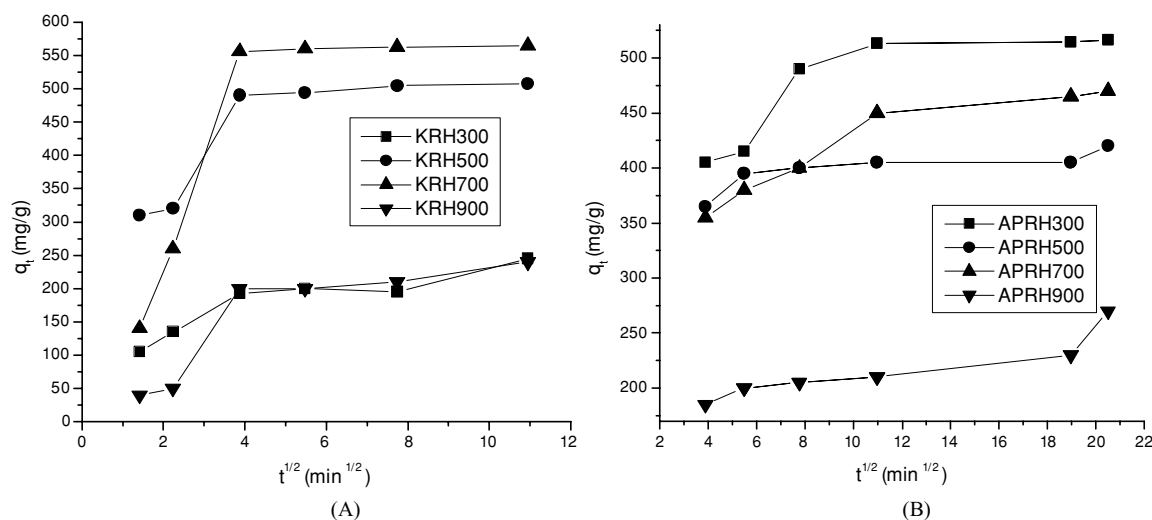


Fig. 5 Fitting of adsorption data with intra particle diffusion model A – KRH and b – APRH

Intra – particle diffusion model

The adsorbate species are transported from the bulk of the solution into the solid phase through intra-particle diffusion/transport process, which is often the rate determining step (Kannan and Sundaram, 2001). This process is explored by the equation

$$q_t = k_p t^{1/2} + c \quad (5)$$

where q_t is the amount of dye adsorbed at time t , and c is the intercept, the value of which gives an idea about the boundary layer thickness. Larger the intercept, the greater is the boundary layer effect. K_p is a coefficient ($\text{mg} \cdot \text{min}^{1/2}/\text{g}$) which reveals the presence of intra-particle diffusion process.

The values of q_t were found to be linearly correlated with values of $t^{1/2}$ (Figure 5). The R^2 values close to unity reveal the presence of intra particle diffusion. All the plots have the same general feature i.e an initial curved portion followed by linear part and a plateau correspond to boundary layer sorption, intra particle diffusion and the equilibrium state respectively. Due to the mass transfer effect, the shape of q_t versus $t^{1/2}$ plot is curved at a small time limit (Annadurai et al., 2002). This also confirms that adsorption of the dye on to the adsorbent is a multi step process, involving adsorption on the external surface and diffusion into the interior. All the steps slow down as the system approaches equilibrium (Bhattacharya and Sarma, 2005). The calculated values of K_p is maximum for KRH700 and mini-

mum for KRH300. This is in good agreement with the values of micro pore fraction. Boundary layer effect is in the order, $\text{KRH700} > \text{APRH300} > \text{KRH500} > \text{APRH700} > \text{APRH500} > \text{KRH900} \approx \text{APRH900} > \text{KRH300}$ which is indicative of the available surface active sites for adsorption. For KRH300, KRH900 and APRH900, boundary layer effect is very small indicating very few surface active sites (Table 4).

The kinetic data obtained from batch studies have been analyzed by applying Lagergren pseudo first order (Ho, 2004) and pseudo second order (Ho and Chiang, 2001) rate equations. The adsorption of dyes from liquid to solid phase can be considered as a reversible reaction with equilibrium established between the two phases. The equations for these models are pseudo first order equation:

$$\text{Log}(q_e - q_t) = \text{log } q_e - [(K_{ad}/2.303)t]. \quad (6)$$

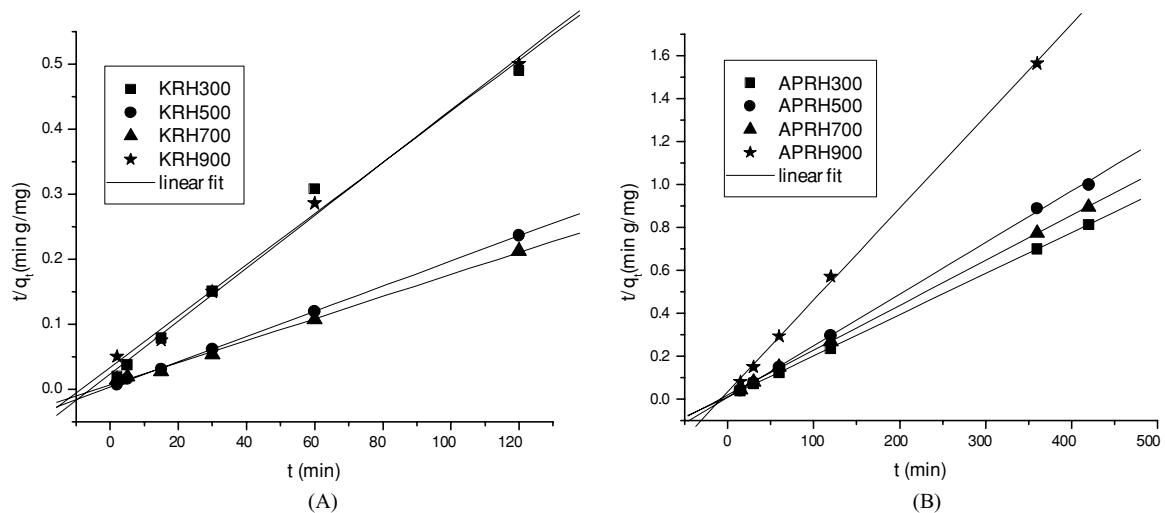
pseudo second order equation:

$$t/q_t = [1/K_{ad}q_e^2] + (1/q_e)t \quad (7)$$

where q_e and q_t are the amount of dye adsorbed per unit mass of the adsorbent (in mg/g) at equilibrium time and the time t respectively. K_{ad} is the rate constant. The validity of the models can be checked from the linear plots of $\text{log}(q_e - q_t)$ versus t and t/q_t versus t . The plot of $\text{log}(q_e - q_t)$ versus t gives very small value of R^2 which indicates that such first order rate expression is not valid to the present system. It can be seen from the Table 5 and Figure 6 that the kinetics of adsorption

Table 5 Parameters of Langmuir, Freundlich, Pseudo 1st & 2nd order models

Samples	Langmuir				Freundlich			1 st order	2 nd order	Rate constant
	<i>b</i>	<i>Q</i> ₀	<i>R</i> ²	<i>R</i> _L	<i>K</i> _f	1/ <i>n</i>	<i>R</i> ²	<i>R</i> ²	<i>R</i> ²	
KRH 300	1.19	178.25	0.9997	0.02	72.11	0.62	1	0.7305	0.9931	0.0007
KRH 500	0.05	689.66	0.9286	0.36	501.65	0.76	0.9993	0.9257	0.9999	0.0012
KRH 700	0.43	369.00	0.9729	0.06	156.19	0.79	0.9901	0.8516	0.9986	0.0004
KRH 900	2.15	96.25	0.9974	0.01	24.94	0.52	0.9997	0.8050	0.9975	0.0004
APRH300	1.10	257.73	0.9779	0.02	438.21	1.50	0.9778	0.8473	0.9999	0.0004
APRH500	1.29	263.16	1.0000	0.02	122.78	0.89	0.9516	0.6359	0.9997	0.0009
APRH700	0.71	147.49	0.9968	0.03	47.09	0.44	0.9617	0.9664	0.9999	0.0003
APRH900	0.33	42.46	0.9999	0.07	33.88	0.07	0.9998	0.9643	0.9996	0.0006

**Fig. 6** Linear fitting of adsorption data with pseudo second order kinetic equation A – KRH and b – APRH

onto the ash follows pseudo second order rate equation with $R^2 \sim 0.99$.

Adsorption data were analyzed with the help of the linear, Langmuir and Freundlich isotherms (Voudrias et al., 2002). The linear isotherm indicates a partitioning process of the solute on to the sorbent. Langmuir isotherm is based on the simple principle where the sorption sites at the interface of the solid are occupied by the adsorbent. It gives an idea about the maximum adsorption capacity. The Freundlich expression is an exponential equation and therefore assumes that as the adsorbate concentration in the solution increases, the adsorption at the surface will also increase. The Freundlich isotherm is equal to linear isotherm when $n = 1$.

The Freundlich equation agrees well with Langmuir over moderate concentration ranges but unlike Freundlich, the Langmuir expression does not reduce to the linear isotherm at lower surface coverage. Both theories

suffer from the disadvantage that equilibrium data over a wide concentration range can not be fitted with a single set of constants. This may be due to the fact that Freundlich isotherm theoretically assumes that an infinite number of adsorption is occurring. But large methylene blue molecules homogenize the rice husk ash surface such that, access to the micro porous structure is restricted and adsorption is limited (Manaskorn et al., 2004). It is reported that Redlich and Peterson isotherm can be used to represent adsorption over a wide range of concentration (Topallar and Bayrak, 1999)

The equations for the three isotherms are as follows:

$$\text{Linear isotherm: } q_e = K_L C_e \quad (8)$$

$$\text{Langmuir isotherm: } C_e/q_e = (1/Q_0 b) + C_e/Q_0 \quad (9)$$

$$\text{Freundlich isotherm: } \log q_e = \log K_f + (1/n) \log C_e \quad (10)$$

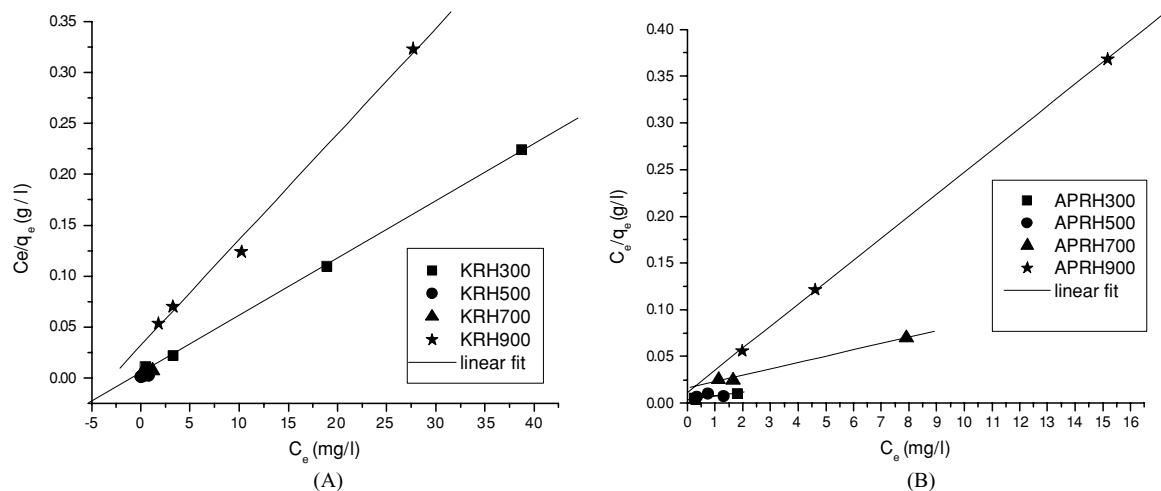


Fig. 7 Linear fitting adsorption data with Langmuir isotherms for A: KRH and B: APRH

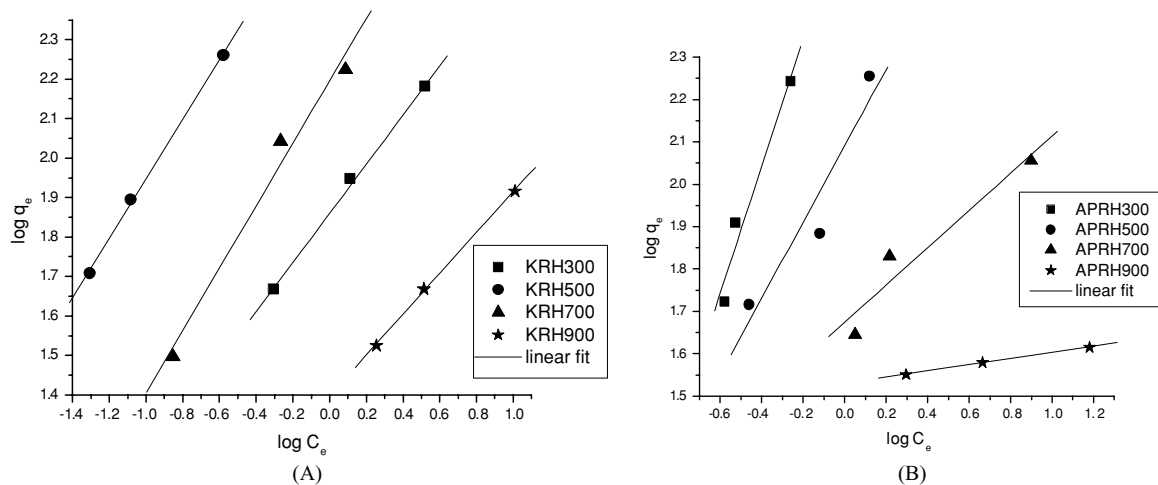


Fig. 8 Linear fitting adsorption data with Freundlich isotherms for A: KRH and B: APRH

where C_e is the equilibrium concentration of dye in solution (mg/l), q_e is the quantity of the dye adsorbed per unit of the sorbent (mg/g) and K_f is a constant. Q_0 is the constant related to the area occupied by a mono layer of sorbent reflecting the sorption capacity (mg/g) which has a greater significance for adsorbent evaluation. b is related to the energy of adsorption and hence is the direct measure of the intensity of adsorption process (l/mg). High value of b implies that strong bonding of dye occurs with the sorbent. K_f represents quantity of dye sorbed in mg/g adsorbent for a unit equilibrium concentration of the dye. High value of K_f shows easy uptake of the dye. The slope $1/n$ measures the surface heterogeneity. Heterogeneity becomes more prevalent as $1/n$ gets closer to zero. For $n = 1$, partition between

the two phases is independent of the concentration and therefore $K_f = K_l$ (linear isotherm). Value for $1/n$ below 1 indicates a normal Freundlich isotherm, while that above 1 is indicative for a co-operative sorption.

In order to decide which type of isotherm fits the experimental data better, the (x/m) was plotted against C_e were plotted for linear, $(\log q_e)$ against $(\log C_e)$ for Freundlich and C_e/q_e against C_e for Langmuir isotherms (Figure 7, 8). The applicability of the model was established from the regression coefficient R^2 . No data satisfies a linear equation, which means that the partition between two phases is dependent on the solution concentration. The R^2 values (goodness of fit criterion) computed by linear regression for the isotherms are represented in the Table 3. From the linear regression

analysis, it is clear that all the products satisfy both Langmuir and Freundlich data to an optimum initial dye concentration (50 mg/l). For higher initial concentrations of the dye, greater variation is shown for both the isotherms. The value of K_f and n are indicative of the adsorption capacity and the degree of non-linearity between solution concentration and adsorption respectively. APRH 300 shows co-operative sorption and all the samples have $1/n < 1$.

The parameters of various isotherms studied can be calculated from the values of the intercept and slope and are given in Table 5. It is significant that the Freundlich plots are nearly parallel to one another with very similar slopes, but the Langmuir plots have converged towards the origin with appreciable difference in slopes. This is due to lack of uniformity in size, shape and surface energy of the ash particles. Even if the number of dye molecules adsorbed on the surface might not be large, the high molecular mass would ensure a substantial monolayer capacity. Further the Langmuir coefficient has sufficiently large values indicating that.

Rice husk ash + Methylene blue \rightleftharpoons [Rice husk ash-Methylene blue Complex] is shifted predominantly towards the right leading to uptake of dye molecules by the RHA surface (Bhattacharya and Sarma, 2005). Thus the rice husk ash has good potential to be used as an adsorbent for the removal of methylene blue from water.

The essential characteristics of Langmuir isotherm can also be described by a dimensionless separation factor R_L which is defined by the following equation,

$$\text{Separation factor } R_L = 1/(1 + bC_0) \quad (11)$$

where C_0 is initial concentration of dye and b is the Langmuir constant. The value of separation factor R_L indicates the nature of the adsorption process as given below.

$R_L > 1$	Unfavorable
$R_L = 1$	Linear
$0 < R_L < 1$	Favorable
$R_L = 0$	Irreversible

In the present study the values of R_L computed are < 1 , indicating that the adsorption process is favorable for all these samples (Vadivelan and Vasanth kumar, 2005). The adsorption behaviour of the dye tends to be of chemical rather than a physical nature. Although more thermodynamic data are needed to determine

whether the mechanism of the process is by physisorption/chemisorption, the R_L values give an approximate indication. The R_L values reported in Table 5 shows that the adsorption is extremely favorable. $R_L \ll 1$ tends to a weak irreversible adsorption ($R_L = 0$). The low values of R_L can explain the high and favorable adsorption of all the samples.

The increasing order of relative adsorption capacity of the ash samples has been calculated separately from Q_0 (Langmuir) and K_f (Freundlich) values and is given below

from Q_0 value:	KRH:-	900 < 300 < 700 < 500;
	APRH:-	900 < 700 < 300 \approx 500;
From K_f value:	KRH:-	900 < 300 < 700 < 500;
	APRH:	900 < 700 < 500 < 300;

The values are found to be in good agreement. From the Q_0 values all ashes except APRH900 & KRH900 can be used as adsorbents for removing methylene blue. KRH500, APRH500 and APRH300 products are showing much higher monolayer capacities. The maximum adsorption capacity Q_0 was shown by KRH 500 and was found to be ~ 690 mg/g. This is comparable with commercially available activated carbons and higher than that of the carbon from rice husk (Bhattacharya and Sarma, 2005; Senthilkumar et al., 2005; Vadivelan and Kumar, 2005). Adsorption capacity values are found to be in good agreement with the surface area and pore volume.

The value of separation factor (R_L) shows that all the ashes except that prepared at 900°C can be used for the removal of methylene blue from aqueous solution. The present study shows considerable potential of rice husk ash as cost effective adsorbent for the removal of basic dyes from aqueous systems. However regeneration of these adsorbents is yet to be studied.

Conclusions

Rice husks from two different locations in India were calcined at different temperatures and the product ashes were characterized for their physical, chemical and morphological properties. Kinetic and equilibrium adsorption studies of methylene blue on the ash samples were conducted. Methylene blue is a cationic dye and adsorbents with neutral or basic pH can favorably remove this dye. All the ash samples except KRH300 are having $\text{pH} \geq 7$. Both pH and pore volume influence the adsorption behavior of the rice husk ash. KRH500

is having maximum surface area and pore volume, pH > 7 and hence highest adsorption capacity. In KRH900 and APRH900, silica is in the crystalline form and these samples are having very low surface area. The N₂ adsorption studies reveal the presence of considerable amount of micro pores in all the products except KRH900, APRH700 and APRH900. Out of the two rice husks, APRH is having higher potassium content and therefore on calcination, the ash shows the presence of entrapped carbon in the product. Three types of isotherms were selected for the adsorption studies namely linear, Langmuir and Freundlich isotherms. From the regression analysis, adsorption data satisfy Langmuir and Freundlich isotherms for all the ash samples ($R^2 \sim 0.99$) but only for a limited range of concentration. This may be due to the fact that Freundlich isotherm theoretically assumes that an infinite number of adsorption is occurring but large methylene blue molecules homogenize the ash surface such that access to the micro porous structure was restricted and adsorption was limited. KRH500 product is having maximum adsorption capacity among the ash samples. The maximum monolayer capacity shown is ~ 690 mg/g. The adsorption process is found to be pseudo second order with intra particle diffusion process as one of the rate determining steps. The value of separation factor (R_L) shows that most of the ash samples under study can be used as effective adsorbents for methylene blue removal from aqueous solutions. Adsorption capacity of rice husk ash is due to the presence of both silica and carbon unlike other low cost lignocellulosic adsorbents where activated carbon is contributing to the adsorption capacity. The rice husk ash can be a potential cost effective adsorbent for the removal of methylene blue dye from aqueous systems.

Acknowledgements The authors are grateful to the Director, RRL(T), for giving permission to communicate this work. Part of the experimental work carried out by Miss. Sandhya, K.S. for her MSc dissertation is also acknowledged. Thanks are also due to Dr. Peter Koshy, Dr. R. Sukumar, Mr. P. Guruswamy, Mr. Veluswamy and Mrs. Viji for SEM, N₂ adsorption datas, XRD, Carbon estimation and IR measurements respectively. One of the authors (PNP) is indebted to DST (Govt.of.India) for financial assistance.

Nomenclature

- R_E Removal Efficiency (%)
 C_0 Initial concentration of the dye mg/l

- C The solution concentration after mg/l adsorption
 m slope of the Log Re versus shaking time (t) curve
 K constant of Log Re versus shaking time (t) curve
 q_t Amount of dye adsorbed at time t ,
 c Intercept of intra particle diffusion
 K_p Intra particle diffusion coefficient (mg. min^{1/2}/g)
 R^2 Linear regression correlation coefficient
 q_e Amount of dye adsorbed per unit mass of the adsorbent (mg/g) at equilibrium time
 q_t Amount of dye adsorbed per unit mass of the adsorbent (in mg/g) at time t
 K_{ad} Rate constant for Lagergren kinetic equation
 C_e Equilibrium concentration of dye in solution (mg/l)
 K_l a constant.
 Q_0 mono layer sorption capacity (mg/g)
 b Langmuir constant (l/mg)
 K_f Quantity of dye sorbed (mg/g) for a unit equilibrium concentration of the dye.
 R_L Separation factor
 MB Methylene blue
 RHA Rice husk ash
 KRH Rice husk from Kerala
 APRH Rice husk from Andhra Pradesh

References

- Al-Degs, Y., M.A.M. Khraisheh, S.J. Allenm, and M.N. Ahmed, "Effect of carbon surface chemistry on the removal of reactive dyes from textile effluent," *Water Research*, **34**, 927–935 (2000).
 Allen, S.J., Q. Gan, R. Matthews, and P.A. Johnson, "Comparison of optimized isotherm models for basic dye adsorption," *Bioresoures Technology*, **88**, 143–52 (2003).
 Annadurai, G., R.S. Juang, and D.J. Lee, "Use of cellulose-based wastes for adsorption of dyes from aqueous solutions," *Journal of Hazardous Material*, **B92**, 263–274 (2002).
 Bhattacharya, K.G. and Arunima Sarma, "Adsorption characteristics of the dye brilliant green on Neem leaf powder," *Dyes and Pigments*, **57**, 211–222 (2003).
 Bhattacharya, K.G. and Sarma Arunima, "Kinetics and thermodynamics of methylene blueadsorption on Neem (*Azadirachta indica*) leaf powder," *Dyes and Pigments*, **65**, 51–59 (2005).
 Chandrasekhar, S., P.N. Pramada, P. Raghavan, K.G. Satyanarayana, and T.N. Gupta, "Microsilica from rice

- husk as a possible substitute for condensed silica fume for high performance concrete,” *Journal of Materials Science Letters*, **21**, 1245–1247 (2002).
- Chandrasekhar, S., K.G. Satyanarayana, P.N. Pramada, P. Raghavan, and T.N. Gupta, “Review-Processing, properties and application of reactive silica from rice husk,” *Journal of Materials Science*, **21**, 3159–3168 (2003).
- Chandrasekhar, S., P.N. Pramada, and L. Praveen, “Effect of organic acid treatment on the properties of rice husk silica,” *Journal of Materials Science*, **40**, 6535–6544 (2005).
- Daifullah, A.A.M., B.S. Girgis, and H.M.H. Gad, “Utilization of agro-residues (rice husk) in small waste water treatment plants,” *Materials Letters*, **57**, 1723–1731 (2003).
- Dogan Mehment and Alkan Mohir, “Removal of MV from aqueous solution by Prlite,” *Journal of Colloid and Interface Science*, **267**, 32–41 (2003).
- Garg, V.K., M. Amita, Rakesh Kumar and Renuka Gupta, “Basic dye (methylene blue) removal from simulated waste water by adsorption using Indian rose wood saw dust: a timber industry waste,” *Dyes and Pigments*, **63**, 243–250 (2004).
- Ho, Y.S., “Citation review of Lagergren kinetic rate equation on adsorption reactions,” *Scientometrics*, **59**, 171–177 (2004).
- Ho, Y.S. and C.C. Chiang, “Sorption studies of acid dye by mixed sorbents,” *Adsorption*, **7**, 139–147 (2001).
- Ibrahim, D.M., S.A. El-Hemaly, and F.M. Abdel-Kerim, “Study of rice husk ash silica by IR spectroscopy,” *Thermo Chimica Acta*, **37**, 307–14 (1980).
- Kannan, N. and M. Meenakshi Sundaram, “Kinetics and mechanism of removal of methylene blue by adsorption on various carbons-a comparative study,” *Dyes and Pigment*, **51**, 25–40 (2001).
- Kannan, N. and M. Meenakshisundaram, “Adsorption of congo red on various activated carbons,” *Water, Air and Soil Pollution*, **138**, 289–305 (2002).
- Krishnarao, R.V., J. Subramanyam, and T. Jagadish Kumar, “Studies on formation of black particles in rice husk silica ash,” *Journal of European Ceramic Society*, **21**, 99–104 (2001).
- Low, K.S. and C.K. Lee, “Quaternized Rice husk as sorbent for reactive dyes,” *Bioresource Technology*, **61**, 121–125 (1997).
- Malik, P.K., “Use of activated carbons prepared from saw dust and rice husk for adsorption of acid dyes: a case study of acid yellow 36,” *Dyes and Pigments*, **56**, 239–249 (2003).
- Manaskorn Rachakornkij, Ruangchaay Sirawan, and Teachakulwiroj Sumate, “Removal of reactive dye from aqueous solution using bagasse fly ash,” *Songklanakarin Journal of Science and Technology*, **26**, 13–24 (2004).
- Mohamed, M.M., “Acid dye removal: A comparison of surfactant-modified mesoporous FSM-16 with activated carbon derived from rice husk,” *Journal of Colloid and Interface Science*, **272**, 28–34 (2004).
- Namasivayam, C., D. Prabha, and M. Kumutha, “Removal of direct red and acid brilliant blue by adsorption onto banana pith,” *Bioresource Technology*, **64**, 77–79 (1998).
- Namasivayam, C. and D. Kavitha, “Removal of congo red from water by adsorption onto activated carbon prepared from coir pith, an agricultural solid waste,” *Dyes and Pigments*, **54**, 47–58 (2002).
- Rahman, I.A. and B. Saad, “Utilisation of Guava seeds as a source of activated carbon for removal of methyl blue from aqueous solution,” *Malaysian Journal of Chemistry*, **5**, 8–14 (2003).
- Sanghi, R. and B. Bhattacharya, “Review on decolorisation of aqueous dye solutions by low cost adsorbents,” *Coloration Technology*, **118**, 256–269 (2002).
- Senthilkumaar, S., P.R. Varadarajan, K. Porkodi, and C.V. Subbuharam, “adsorption of methylene blue onto jute fibre carbon: kinetics and equilibrium studies,” *Journal of Colloid and Interface Science*, **284**, 78–82 (2005).
- Sumanjit and N. Prasad, “Adsorption of dyes on rice husk ash,” *Indian Journal of Chemistry*, **40A**, 388–391 (2003).
- Topallar, H. and Y. Bayrak, “Investigation of adsorption isotherms of myristic, palmitic and stearic acids on rice hull ash,” *Turk Journal of Chemistry*, **23**, 193–198 (1999).
- Vadivelan, V. and K. Vasanth Kumar, “Equilibrium, kinetics, mechanism and process design for the sorption of methylene blue onto rice husk,” *Journal of Colloid and Interface Science*, **286**, 90–100 (2005).
- Valix, M., W.H. Cheung, and G. McKay, “Preparation of activated carbon using low temperature carbonization and physical activation of high ash raw bagasse for acid dye adsorption,” *Chemosphere*, **56**, 493–501 (2004).
- Voudrias, E., K. Fytianos, and E. Bonzani, “Sorption-Desorption isotherm of dyes from aqueous solutions and waste waters with different sorbent materials,” *Globel Nest: The International Journal*, **4**, 75–83 (2002).
- Waranusantigul, P., P. Pokethitiyook, M. Kruatrachue, and E.S. Upatham, “Kinetics of basic dye (Methylene blue) biosorption by giant duckweed (*Spirodela polyrrhiza*),” *Environmental Pollution*, **125**, 385–392 (2003).
- Yupeng Guo, Zhang Hui, and Tao Nannan, “Adsorption of Malachite green and iodine on rice husk based porous carbon,” *Materials Chemistry and Physics*, **82**, 107–115 (2003).
- Yupeng Guo, Yang Shaofeng, Yu Karfeng, Zhao Jingzhe, Wang Zichen and Xu Hongding, “The preparation and mechanism studies of rice husk based porous carbon,” *Materials Chemistry and Physics*, **74**, 320–323 (2004).